SRL-0112-RN

AR-008-151

DEPARTMENT OF DEFENCE

DEFENCE SCIENCE AND TECHNOLOGY ORGANISATION

SURVEILLANCE RESEARCH LABORATORY

SALISBURY, SOUTH AUSTRALIA

RESEARCH NOTE
SRL-0112-RN

SENSOR MODELLING FOR THE 'CYCLOPS' FOCAL PLANE DETECTOR ARRAY BASED TECHNOLOGY DEMONSTRATOR

by

G.V. Poropat

December 1992

DISCLAIMER NOTICE

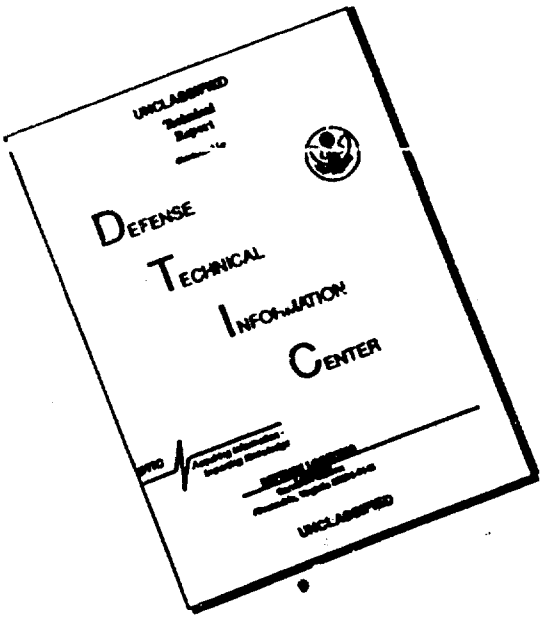

THIS DOCUMENT IS BEST QUALITY AVAILABLE. THE COPY FURNISHED TO DTIC CONTAINED A SIGNIFICANT NUMBER OF PAGES WHICH DO NOT REPRODUCE LEGIBLY.

AR-008-151

DEPARTMENT OF DEFENCE

DEFENCE SCIENCE AND TECHNOLOGY ORGANISATION

SURVEILLANCE RESEARCH LABORATORY

SALISBURY, SOUTH AUSTRALIA

OPTOELECTRONICS DIVISION

RESEARCH NOTE
SRL-0112-RN

SENSOR MODELLING FOR THE 'CYCLOPS' FOCAL PLANE DETECTOR ARRAY BASED TECHNOLOGY DEMONSTRATOR

by

G.V. Poropat

SUMMARY

The Surveillance Research Laboratory of the DSTO has developed a technology demonstrator utilising an infrared focal plane detector array to assess the feasibility of using large scale infrared detector arrays for ADF applications. The imaging sensor which has been developed requires no scanning mechanism and uses an array of mercury cadmium telluride detectors sensitive to radiation in the 8 μm to 12 μm spectral region to produce an image. The sensor was tested in a series of airborne trails and the results obtained from these trials will be used to evaluate the performance of focal plane detector array based systems. A mathematical model of the sensor has been used to evaluate the performance of the sensor. The mathematical model has been developed to meet the requirements imposed by analysis of the performance of this sensor. The model is based on the description of the operation of the elements of the detector array as photon counters. A description of the model used for the analysis of the data obtained using the sensor is presented here.

POSTAL ADDRESS: Director, Surveillance Research Laboratory, PO Box 1500, Salisbury, South Australia, 5108.

CONTENTS

FIGURES

THIS IS A BLANK PAGE

ABBREVIATIONS

ADF	Australian Defence Forces
CMT	Cadmium Mercury Telluride
FPDA	Focal Plane Detector Array
IFOV	Instantaneous field of view
IRFPDA	Infrared Focal Plane Detector Array
LWIR	Long-Wave Infrared
MCT	Mercury Cadmium Telluride
MTF	Modulation Transfer Function
PSF	Point Spread Function
SRL	Surveillance Research Laboratory
SNR	Signal to noise ratio

THIS IS A BLANK PAGE

1 INTRODUCTION

Optoelectronics Division of the Surveillance Research Laboratory (SRL) has developed an experimental infrared sensor system which utilises a large scale focal plane detector array (FPDA). The sensor system operates in the long-wave infrared (LWIR) spectral region. The detector array consists of photodiodes fabricated on a mercury cadmium telluride (HgCdTe, MCT or CMT) wafer with readout electronics fabricated on a silicon wafer to which the detector array is bonded. The technology demonstrator has been used to test the capabilities of infrared systems utilising FPDAs for ADF applications.

Detection of a target by a FPDA based imaging sensor is based on the generation of electrical signals by elements of the detector array as a result of the detection of infrared radiation emitted by the target. These signals must be reliably identified in the presence of system noise, noise generated external to the sensor and background signals.

The prediction of the performance of the sensor system requires a mathematical model of the sensor system, the target and the operating environment which will permit the estimation of the differential target to background signal and the noise signal in order to predict detection ranges for a variety of targets and operating conditions. The model must take into account the nature of the infrared emission from the target, the emission and transmission of infrared radiation by the atmosphere and the processes occurring in the sensor system which affect detection of the target including temporal and spatial noise and other sources of signal degradation. To meet the needs of the performance analysis of the sensor and associated image and data processing systems, the model presented here provides an estimate of the differential target to background signal to noise ratio.

The model accounts for the spectral response of the sensor system (including optical components), the optical resolution of the sensor, the spectral responsivity of the elements of the detector array and the noise processes which ultimately limit the performance of the sensor. The spectral properties of the emission from the target are assumed to be those of a black body radiator and the emission and transmission of the atmosphere are calculated using the computer program LOWTRAN.

The calculation of the performance of the infrared system in the model is performed in photon units since the photovoltaic detectors used are photon counters. The infrared emission from the target is thus calculated as a spectral distribution of the emission of photons. The computer program LOWTRAN produces, as output, estimates of the emission from the atmosphere which are calculated in watts and presented as a spectral distribution in cm^{-1}. For use with the model developed here, these data are converted to photon units and the spectral distribution is interpolated and expressed in equal wavelength intervals.

The format of the model allows the use of detector noise models which reflect the nature of the noise processes in the detector and charge storage mechanisms for staring arrays. With this format, the model readily includes the effects of internal stray fluxes which have been measured as a photon generated carrier count. The model described here has been developed to meet the need for modelling an FPDA based sensor for a restricted range of applications and does not include effects such as those arising from charge transfer inefficiencies in the readout circuitry.

The performance of the HgCdTe FPDA based sensor is limited by the nonuniformity of the responsivities of the detectors comprising the array and by the architecture of the array which operates in a line scanned equivalent mode. The model has been developed so as to allow the effects of nonuniformities in responsivity to be included in the calculation of the noise signals which affect the probability of detection of a target.

The model uses a simple approximation to the source. The approximation is based on knowledge of the sources expected to be imaged by the sensor. The model does not provide any estimate of the probability of detection of a source which might be observed when the sensor is used to present images to an observer since, in operation, the data produced by the sensor will be processed by an automatic target detection system.

The probability of detection of an object in the field of view of an imaging sensor is a complex function of the optical system and detector array architecture including the detector size and spacing. The model described here incorporates the effects of these system elements on the signals obtained from the detector array, and thus the detection process. The model is used to predict the performance of an autonomous target detection system utilising an infrared imaging sensor. The sensor incorporates an infrared focal plane detector array operating in a staring mode. The approach described here specifically accommodates the spatial noise in the image where the spatial noise arises from the nonuniformity of the responsivities of the detectors in the array.

The model has been developed using the photon spectral sterance (or radiance), $L_{q\lambda}$, rather than the spectral radiance, L_{λ}, since the detectors used are photon counters. The photon form of Planck's law is derived readily from the energy form commonly used but is more naturally derived directly from the physics of the emission of radiation[1]. The use of this form of Planck's law removes the requirement to explicitly convert from energy units to photon counts. This approach is logically consistent when dealing with a detector which operates purely as a photon counter.

The approach used here thus differs from an approach based on the energy form of Planck's law as used by Cutten and Findlay[2] since such an approach requires transformation of the detector energy responsivity to a photon responsivity. In addition, the wide variation of the spectral responsivities of the detectors in the array used and the varying spectral characteristics of the atmosphere in the experiments undertaken makes the exact formalism used here preferable to the use of 'band average' or 'spectrally weighted' quantities since such quantities may not reflect the spectral variations observed.

The detector figure of merit, D*, has not been used in the analysis presented here. The use of D*, which embodies concepts of signal bandwidth and noise power spectral density in the estimation of the performance of infrared systems, is common practice in the analysis of scanned infrared sensor systems. This is an approach which is inherently difficult to apply to a 'staring' detector array since the development of D* is based on continuous time processes more suited to scanned detectors with continuous readout. An assumption which has been made in the development of this model is that the temporal variation in the image flux distribution is negligibly small. This assumption removes the necessity to consider the detector as an element in a linear continuous time signal processing system and allows a treatment of the noise processes observed with the sensor used which is more closely related to measurable quantities such as the number of noise electrons per pixel.

2 BASIS OF THE MODEL

The radiation from the target is treated as blackbody radiation from a source of known extent and uniform distribution at a known temperature. The spectral distribution of the radiation from the source is thus given by Planck's law. The radiation detected by the elements of the focal plane array consists of the radiation from the target after its spectral distribution and amplitude have been modified by transmission through the atmosphere and any optical components combined with radiation emitted by the atmosphere, radiation from components of the system and any other stray radiation.

The intensity of the flux distribution (the image) at any point on the focal plane of an imaging system produced by a scene is determined by the scene characteristics (the distribution and temperatures of emitters in object space) as well as the properties of the atmosphere and the sensor system.

For complex scenes, the spatial distribution of the photon flux on the focal plane will be difficult to predict and will be dependent on the effects of optical blurring on the undistorted image of the scene. Blurring of

the image arises from transmission of the radiation through the atmosphere, from sensor motion and from the optical system of the sensor. In the analysis presented here blurring due to the atmosphere is not considered and the assumption is made that there is no relative motion between the target and the sensor; ie, the target image on the focal plane is not blurred due to sensor or target motion. The optical system degrades the image produced due to its limited spatial bandwidth and the effect of this limited spatial bandwidth is to produce smearing of the image of the scene features on the focal plane.

It can be shown that, if an extended uniform source in the object space of an infrared imaging system produces an image on the focal plane which is much greater in extent than the point spread function (PSF) on the focal plane, blurring caused by the optical system does not reduce the image contrast at the centre of the feature. For this case, blurring will affect only the irradiance distribution at the edges of the image of the object on the focal plane relative to an ideal image. For extended objects, the variation of target to background contrast with range is primarily dependent on the spectral characteristics of the target and the atmosphere. The photon flux distribution on the focal plane arising due to an extended source can be estimated in a straightforward manner without the necessity to accommodate the effects of diffraction or other processes that degrade the resolution of the image.

The photon flux incident on the detector when an extended target is present depends on the range to the target, which determines atmospheric transmission from the target and the emission from the atmosphere along the line of sight to the target, as well as the target emission characteristics. The atmospheric effects are accommodated through the use of atmospheric emission and transmission data calculated by the computer program LOWTRAN.

The effect of blurring due to the optical system when the apparent size of an object is small; ie, the extent of the target image on the focal plane is comparable to, or smaller than, the system PSF is to reduce the maximum intensity of the photon distribution on the focal plane due to the target in comparison to the intensity that would be observed from an extended source of the same radiance. This reduces the target to background contrast when a 'small' target is viewed against a uniform background and thus reduces the detection probability of small targets.

The apparent size of the object and thus the maximum intensity of the photon distribution due to the object on the focal plane decreases with increasing range. Thus the detection probability will reduce with range due to the combination of apparent target size and atmospheric effects. The reduction in detection probability with decreasing apparent target size may increase faster with increasing range than that which would be predicted as arising from the effects of atmospheric emission and transmission alone. The model developed here accounts for the effects of target size and range and the characteristics of the optical system.

For any line of sight which does not intersect the earth's surface the photon flux incident on the detector in the absence of a target is determined entirely by the atmospheric emission along the line of sight and any stray flux; eg, flux from the optical components. The line of sight will intersect many levels of the atmosphere and the apparent radiometric temperature observed along the line of sight cannot be directly related to atmospheric temperature. The model can be used to determine apparent background temperature.

The sensor model accounts for:

- background emission from the atmosphere along the line of sight,
- emission from the atmosphere between the target and the sensor along the line of sight,
- emission from the target,
- the size of the target,
- target range,
- the focal length of the optical system,

- the PSF of the optical system,
- the spectral transmission of the optical system,
- the spectral response of the detectors,
- the charge transfer efficiency on the focal plane, and
- the detector size and spacing.

The model also accounts for

photon noise,

detector temporal noise, and

spatial noise due to the nonuniformity of the responsivity of the elements of the FPDA.

The model does not attempt to predict detection ranges which would be achieved by displaying the image to an observer. The model provides an estimate of image signal to noise ratio which can be used to predict the target detection range for an automated processor which might for instance use an 'M out of N' track initiator for target detection. An 'M out of N' track initiator spatially correlates M threshold exceedances in N frames. A detection model for an automated processor, based on thresholding followed by an 'M out of N' track initiator, can be used to define detection ranges using the signal to noise ratio data obtained using the model presented here.

3 FORMATION OF AN IMAGE OF AN OBJECT ON THE FOCAL PLANE

Over a limited field angle, the formation of the image of a feature in the object space of an imaging system on the focal plane of the system can be described using the two dimensional convolution of the undegraded image of the feature on the focal plane as would be formed by an idealised lens and the system PSF on the focal plane[3]. The PSF of the imaging system and the distribution of emitters in object space determine the distribution of the image flux on the focal plane which is mathematically described by

$$z(x,y) = \int_{-\infty}^{\infty}\int_{-\infty}^{\infty} s(\tau,\sigma).h(x-\tau,y-\sigma)d\tau d\sigma \qquad (1)$$

where $z(x,y)$ is the image flux distribution on the focal plane, $s(x,y)$ is the undegraded image flux distribution on the focal plane (the image distribution which would be produced by an idealised blur free lens) and $h(x,y)$ is the system PSF on the focal plane.

In the spatial frequency domain, optical systems are band limited by the diffraction which occurs due to the finite extent of the collecting aperture. The diffraction limited PSF of a distortionless optical system with a circular aperture will have the form of a Bessel function of the first kind. Optical systems may not be diffraction limited and the effects of blurring can be conveniently modelled in many cases by assuming that the system has a PSF which has the form of the Gaussian function. The error which results from using a Gaussian PSF as an approximation to the diffraction limited PSF for a system with a circular aperture is negligible and, for ease of calculation, a PSF of this form will be assumed in the analysis presented here.

The Gaussian PSF has a Gaussian modulation transfer function (MTF) which is not band limited. The one dimensional Gaussian MTF has the general form

$$\exp(-\frac{\omega^2}{\alpha}) \quad \text{or more conveniently} \quad \exp(-\frac{\omega^2}{4\alpha}) \quad \text{which has a PSF of the form } \exp(-\alpha x^2)$$

where ω is spatial frequency. The units for ω used here are radians length^{-1} on the focal plane. Line pairs length^{-1} are sometimes used to specify spatial frequency, however this terminology is a descriptor for bar spacing for a resolution chart and is not appropriate for the analysis here. The Gaussian MTF of the form used here is unity at a spatial frequency of zero and has a line spread function

$$\sqrt{\frac{\alpha}{\pi}}\exp(-\alpha.x^2)$$

on the focal plane. The two dimensional symmetric Gaussian point spread function is

$$\frac{\alpha}{\pi}.\exp(-\alpha.(x^2+y^2))$$

The two dimensional form of the PSF has been used with two source distributions to derive expressions for the focal plane image flux distributions of the images of these sources in the model. The target distributions used are a square target and a circularly symmetric target. These distributions are described by

$$s(x,y) = \text{rect}(x.\beta).\text{rect}(y.\beta) \qquad (2)$$

where

$\text{rect}(x.\beta) = 1.0$ if $|x.\beta| \le 0.5$ and

$\text{rect}(x.\beta) = 0.0$ otherwise for the square target

and

$$s(x,y) = 1.0 \quad \text{if } (x^2+y^2) < 0.5.\beta^{-1} \text{ and} \qquad (3)$$

$$s(x,y) = 0.0 \quad \text{if } (x^2+y^2) > 0.5.\beta^{-1}$$

for the circular target.

For both these distributions, the amplitude of the distribution is unity. The source functions have been defined so that as β increases the extent of the target distribution decreases. The effect of using these distributions is that, as the target size increases the total emission from the target increases.

For a square target, the image distribution formed on the focal plane of a system with a Gaussian PSF is

$$z(x,y) = \frac{\alpha}{\pi}\int_{-\infty}^{\infty}\int_{-\infty}^{\infty}\exp(-\alpha((x-\tau)^2+(y-\sigma)^2).\text{rect}(\tau.\beta).\text{rect}(\sigma.\beta)d\tau d\sigma \qquad (4)$$

which can be expressed as

$$z(x,y) = \frac{\alpha}{\pi}\int_{\frac{-0.5}{\beta}}^{\frac{0.5}{\beta}}\exp(-\alpha.(x-\tau)^2)d\tau.\int_{\frac{-0.5}{\beta}}^{\frac{0.5}{\beta}}\exp(-\alpha.(y-\sigma)^2)d\sigma \qquad (5)$$

This can be further simplified to

$$z(x,y)=\frac{1}{2\pi}\int_{\sqrt{2\alpha}(x-\frac{0.5}{\beta})}^{\sqrt{2\alpha}(x+\frac{0.5}{\beta})}\exp(-\frac{\tau^2}{2})d\tau.\int_{\sqrt{2\alpha}(y-\frac{0.5}{\beta})}^{\sqrt{2\alpha}(y+\frac{0.5}{\beta})}\exp(-\frac{\sigma^2}{2})d\sigma \qquad (6)$$

which uses the standard form of the error function.

The image distribution formed on the focal plane by a circular target is

$$z(x,y)=\frac{\alpha}{\pi}\int_{-\infty}^{\infty}\int_{-\infty}^{\infty}\exp(-\alpha((x-\tau)^2+(y-\sigma)^2)).s(\tau,\sigma).d\tau.d\sigma \qquad (7)$$

where $s(\tau,\sigma)$ is the circular target distribution defined previously. For the circular target, the image distribution on the focal plane can be expressed in polar coordinates as

$$z(r,\phi)=\frac{\alpha}{\pi}\int_{0}^{2\pi}\int_{0}^{\frac{0.5}{\beta}}\exp(-\alpha(r^2+\tau^2-2.r.\tau.\cos(\phi-\theta)))d\tau.d\theta \qquad (8)$$

which does not have a closed form solution. To simplify this expression the term

$$\int_{0}^{2\pi}\exp(\kappa\cos(\theta))d\theta$$

can be approximated (empirically) as

$$\int_{0}^{2\pi}\frac{\exp(\kappa)+\exp(-\kappa)}{2}d\theta$$

The accuracy of the approximation decreases as β increases. Using this approximation the system response to a circular target in the field of regard (ie the flux distribution on the focal plane produced by a circular target) can be expressed as

$$z(r)=\alpha\int_{0}^{\frac{0.5}{\beta}}\exp(-\alpha(r^2+\tau^2)).(\exp(2\alpha\tau)+\exp(-2\alpha\tau))d\tau. \qquad (9)$$

It should be noted that the accuracy of the approximation is exact for r equal zero. As r deviates from zero the accuracy of the approximation decreases rapidly as α increases.

4 REDUCTION OF IMAGE AMPLITUDE WITH THE DIMENSION OF AN OBJECT IMAGE ON THE FOCAL PLANE

The analysis of the formation of the image on the focal plane predicts that with an increase in β, corresponding to a reduction in the extent of the image on the focal plane, the peak amplitude of the image will decrease for images less than a critical size which is of the order of the system PSF.

To demonstrate the effect of the blurring produced by a Gaussian PSF on the image produced on the focal plane by a line source, the one dimensional form of the PSF was used. The line source distributions used are characterised by an amplitude of unity and the form rect(x.β); the spatial extent of the source decreases as β increases. Figure 1 shows the focal plane image distributions for uniform line source distributions which have a spatial extent on the focal plane of 0.177, 0.707 and 7.07 times the half width of the system PSF on the focal plane. The half width of the PSF is defined by the distance from the PSF maximum to the 1/e point, $\alpha^{-0.5}$, in this case 1.414. These distributions correspond to values of β of 2α, 0.5α and 0.05α respectively.

The reduction in the peak of the image distribution with reduction in the extent of the source is readily apparent in Figure 1; The data for this figure have been calculated using the one dimensional form of equation (6). It can be seen that as the apparent object size is reduced from a size which is much larger than the PSF (an extended object) to a size which is comparable to or smaller than the PSF, the target to background contrast is reduced.

As shown previously, an analytical solution to the convolution integral in two dimensions exists only for the simplest geometries of the system PSF and the target. The model described uses an idealised Gaussian PSF and two simple target geometries, a square target and a circular target, both of uniform amplitude. For square or circular targets whose image on the focal plane has a spatial extent smaller than the system PSF the reduction in the peak image amplitude using the two dimensional analysis is greater than that predicted for a line source, ie the one dimensional case. For a typical infrared lens with α of $1.56*10^{10}$ m^2 the calculated peak image amplitudes for a line source, a square source and a circular source of 5 metres extent (width, length of side and diameter respectively) at a range of 20 km are 0.731, 0.534 and 0.457 of the peak amplitude of an extended source of the same radiance respectively.

The difference observed in the peak amplitudes of the images for the square source and the circular source when the image extent is not significantly larger than the PSF is attributable to the larger area of the square source with the source function definitions used. The source area determines the total flux emitted and thus the larger area of a rectangular source produces a slightly greater image amplitude. The observed reduction in the peak amplitude of the image distributions for these sources when compared to the line source is also a function of the larger area of the line source contributing to the image flux distribution.

It is obvious from these results that, unless the target geometry and the effects of blurring of the target image for targets with small apparent sizes at long ranges are accounted for, estimates of the target to background contrast for such targets will be optimistic.

Figure 2 illustrates the shape of the ideal flux distribution on the focal plane due to a square target when there is no blurring. Figure 3 shows the flux distribution from the same target after blurring due to the optical system. The calculation has been performed using the parameters above and the peak signal level of the blurred image is 0.534 of the signal peak amplitude of the original target distribution.

In the model developed, a square target distribution is generally assumed. This has the advantage of requiring significantly less computational effort than that required for a circular target although a circular target distribution can be used. The use of the square target distribution provides a reasonable estimate of the effect of apparent target size on target to background contrast in two dimensions and a simple correction can be made, if necessary, to improve the estimate as an approximation to the case for a circular target.

5 INTEGRATION OF IMAGE PLANE PHOTON IRRADIANCE BY A PHOTODETECTOR

The signal obtained from the detector results from the generation of carriers arising from the absorption of the photon flux over the active area of the detector. The observed reduction in target to background contrast will depend on the relationship between the spatial extent of the target distribution, the system PSF, the detector active area and the spacing of detectors on the focal plane.

In the case of a staring array, assuming that the temporal variation in the image flux distribution is small, the number of carriers generated is obtained from the spatial integral of the image flux distribution over the active area of the detector for a time which is often, although not always, the frame time. For a scanning system, spatial changes in a feature can result in temporal variations in the image flux integrated by the detector during the scan period. For a scanning system, the temporal variation of the image flux as it is scanned across the detector may be significant and the time response of the detector and signal conditioning electronics must then be taken into account.

The tradeoffs between optical system design and spatial sampling on the focal plane will, in part, determine the probability of detection of a target. The optical system design and array geometry are critical system design factors which have to be optimised for maximum performance in terms of detection range. The analysis presented here assumes that the image of the source is, in all cases, centred on the detector and thus provides an estimate of the maximum target signal and the maximum target to background signal to noise ratio. The spatial dependence of these quantities is beyond the scope of this report and is not addressed here.

The model described here provides a capability to predict the performance of imaging systems using staring FPDAs only. No attempt is made to extend the model to accommodate scanning systems.

The detector array used is comprised of detectors which have been fabricated with a plated through contact to the substrate formed over a hole which has been machined in the detector substrate. The detector sensitive area is therefore an annulus. For the simple case of imaging a unit impulse, the PSF is circularly symmetric and has the form (in polar coordinates) of $\exp(-\alpha.r^2)$ when centred on the coordinate system origin.

The number of carriers generated in a detector is dependent on the total photon flux incident on the detector. When imaging a point source, the photon flux incident on the detector is given by the integral of the PSF over the sensitive area of the detector. If the centre of the PSF and the centre of the detector are coincident on the focal plane then, using polar coordinates for any general point (x,y) in the coordinate system, the integral of the PSF over the sensitive area of the detector is given by

$$\frac{\alpha}{\pi}.\int_{r_1}^{r_2}\int_{0}^{2\pi}\exp(-\alpha.r^2)r.d\theta.dr \qquad (10)$$

where r_1 and r_2 are the inner and outer radii, respectively, of the sensitive region of the detector. The output signal for a detector whose centre is aligned with the centre of the image of a square source is proportional to the number of carriers generated by the incident flux which is given by

$$n = 2\pi.\int_{r_1}^{r_2}\eta.\phi.z(r.\cos\theta, y.\sin\theta)r.d\theta.dr \qquad (11)$$

where η is the average detector quantum efficiency, or more correctly the average detector photon collection efficiency. The more general response term, photon collection efficiency, can be used to include

the effects of surface and other reflection coefficients as well as the detector quantum efficiency. The term z(x,y) is the normalised flux distribution

$$z(x,y) = \frac{1}{2\pi} \int_{\sqrt{2\alpha}(x-\frac{0.5}{\beta})}^{\sqrt{2\alpha}(x+\frac{0.5}{\beta})} \exp(-\frac{\tau^2}{2}) d\tau . \int_{\sqrt{2\alpha}(y-\frac{0.5}{\beta})}^{\sqrt{2\alpha}(y+\frac{0.5}{\beta})} \exp(-\frac{\sigma^2}{2}) d\sigma \qquad (12)$$

as derived previously, and ϕ is the photon flux which would be incident on the focal plane due to the presence of an extended source in the field of view. The function ϕ is a complex function of the spectral response of the system and the spectral characteristics of the source.

6 TARGET TO BACKGROUND CONTRAST AND SIGNAL TO NOISE RATIO FOR EXTENDED OBJECTS

For an extended object, the image produced by the object on the focal plane of the imaging system is much larger than the PSF of the imaging system. As has been shown, in this case the flux distribution of the image of a uniform source produced on the focal plane is uniform over most of the extent of the image and spatial variation of the image of the feature can be ignored when estimating the target to background contrast.

The apparent size of a source in the object space is dependent on the physical dimensions of the source and the distance from the source to the sensor. For a given source, the apparent size will obviously decrease as the distance between the source and the sensor increases. When the apparent size of a source decreases to an extent where the image of the source on the focal plane is not significantly greater than the system point spread function, the target to background contrast will be reduced as a result of further reduction in the apparent size of the source. The estimation of the target to background contrast for targets of small apparent size is accomplished by calculation of the target to background contrast for an extended source and then applying the necessary corrections to account for the reduced apparent size of the target.

The target to background contrast for an extended object is obtained from estimates of the infrared photon flux on the focal plane due to emission from the feature of interest and the photon flux on the focal plane due to emission from the background. The target to background contrast is then given by the standard expression

$$C = \frac{\phi_t - \phi_b}{\phi_b} \qquad (13)$$

where ϕ_t is the target photon flux and ϕ_b is the background photon flux.

The 'target' flux incident on the collecting aperture of the optical system consists of three components: the emission from the target (attenuated by the atmosphere through which the radiation passes to reach the sensor), the emission from the atmosphere between the target and the sensor in the direction of the sensor incident on the aperture and any stray flux. Stray fluxes incident on the collecting aperture are normally ignored. The 'target' flux incident on the detector consists of these component fluxes modified by the spectral transmission of the optical components of the system and added to by any internal stray fluxes from sources such as the components of the sensor.

The background flux and the target flux incident on the collecting aperture are both reduced by the wavelength dependent transmission of the sensor optics. The apparent target contrast may be further

reduced by internal emission from the components of the sensor but this flux will be treated as a constant in the following analysis.

We assume that the target is a black body at a known temperature. Thus the target emission can be calculated using Planck's law which gives the spectral distribution of the photon emission per steradian per unit wavelength interval from a black body at temperature T as[1]

$$L_{q,\lambda}(\lambda,T)=\frac{2.c}{\lambda^4.(\exp(\frac{h.c}{\lambda.kT})-1)}[\text{photons.m}^{-2}.\text{sec}^{-1}.\text{m}^{-1}.\text{sr}^{-1}] \quad (14)$$

Ignoring atmospheric transmission and emission, the irradiance per wavelength increment $d\lambda$ collected at the entrance aperture of area A_c of an imaging system and which will be incident on a detector on the focal plane of the system (where the projected detector instantaneous field of view is Ω) is

$$\phi_{q,\lambda}(T)=\frac{2.c.A_c.\Omega}{\lambda^4.(\exp(\frac{h.c}{\lambda.k.T})-1)}.[\text{photons.sec}^{-1}.\mu\text{m}^{-1}]. \quad (15)$$

With some simplifying assumptions[1] (conservation of the $A.\Omega$ product), this can be expressed in terms of the detector 'area' and the F/number of the optics. Neglecting atmospheric emission and accounting for atmospheric transmission and the transmission of the optics of the system, the flux incident on an area of the focal plane, A_d the detector active area, due to the emission from an extended source of temperature T which completely fills the detector instantaneous field of view, is then[1]

$$\phi_q(T)=\frac{A_d.\pi}{4.F^2}\int_{\lambda_o}^{\lambda_{co}} L_{q,\lambda}(\lambda,T).\tau_O(\lambda).\tau_A(\lambda)d\lambda[\text{photons.sec}^{-1}] \quad (16)$$

where $\tau_O(\lambda)$ and $\tau_A(\lambda)$ are the spectral transmissions of the system optics and the atmosphere respectively and A_d is the detector area, F is the F/number of the optical system, λ_{CO} is the long wavelength cutoff of the system spectral response (which is often determined by the detector cutoff wavelength) and λ_O is the short wavelength limit of the system response. Atmospheric emission and transmission are complex functions of the environment and are calculated for the analysis presented here using the computer program LOWTRAN.

The photon flux incident on the detector is converted to an electrical signal by the generation of carriers as a result of the absorption of the photons in the detector. The number of carriers generated in a detector by the flux from the target is dependent on the detector spectral photon collection efficiency, $\eta(\lambda)$, and is

$$n_t=\frac{A_d.\pi}{4.F^2}\int_{\lambda_o}^{\lambda_{co}}\eta(\lambda).L_{q,\lambda}(\lambda,T).\tau_O(\lambda).\tau_A(\lambda)d\lambda[\text{sec}^{-1}] \quad (17)$$

The flux incident on the focal plane from the target is added to by the flux emitted along the line of sight by the intervening atmosphere between the sensor and the target; this flux is also collected by the sensor. The number of carriers generated by the emission from the atmosphere along the line of sight to the target is given by

$$n_a = \frac{A_d.\pi}{4.F^2}\int_{\lambda_0}^{\lambda_\infty}\eta(\lambda).\varepsilon_a(\lambda).\tau_O(\lambda)d\lambda[sec^{-1}] \quad (18)$$

where $\varepsilon_a(\lambda)$ is the emission from the atmosphere between the target and the sensor observed along the line of sight.

The background flux incident on the focal plane in the absence of a target in the field of view is determined by the total atmospheric emission along the line of sight and generates carriers in the detector at a rate of

$$n_b = \frac{A_d.\pi}{4.F^2}\int_{\lambda_0}^{\lambda_\infty}\eta(\lambda).\varepsilon_b(\lambda).\tau_O(\lambda)d\lambda[sec^{-1}] \quad (19)$$

where $\varepsilon_b(\lambda)$ is the spectral radiance of the atmosphere observed along the line of sight.

The calculation of the photon flux emitted by the target is undertaken in terms of the numbers of photons emitted rather than the energy emitted. The photon radiance is calculated as the number of photons per unit wavelength (in metres) and to maintain consistency, the spectral transmission and emission of the atmosphere are converted to these units with the same wavelength dependency.

Using a spline interpolation technique, the data obtained from LOWTRAN is converted from energy emitted in a frequency interval, in units of cm^{-1}, to photons emitted in a wavelength interval of 0.01 μm or 0.05 μm. The units used in the LOWTRAN calculations, $W/(cm^2.steradian.cm^{-1})$, are then converted to unit of photons / $(m^2.steradian.m^{-1})$. The first step in this conversion is the calculation of the number of photons in each (unequal) LOWTRAN frequency interval which is done by dividing each energy value by the photon energy at that wavelength. The emission per unit area is then converted from units of cm^2 to units of m^2.

The unit of wavenumbers, cm^{-1}, is $2.998.10^{10}$ Hz and the LOWTRAN data is converted to emission in a frequency interval measured in hertz by scaling directly. The data is then converted to emission per wavelength interval of metres with the conversion factor $c.\lambda^{-2}$. The atmospheric emission data along the line of sight between the target and the sensor and the atmospheric emission data along the same line of sight for no target (ie the background emission in the absence of a target) are converted by applying the same algorithm.

For detectors with charge storage, the carriers generated within the detector are integrated for some defined period before being read out to a signal conditioning circuit. Some proportion of the background signal is usually subtracted from the overall signal and, if the image is displayed, the displayed target to background contrast is then a function of the amount of the background signal or pedestal which has been removed and a function of the signal conditioning and display parameters.

In the model described here, we define the image signal to noise ratio (SNR) as the ratio of the differential target to background signal to the detector noise at the output of the detector. For systems utilising an image processor to detect targets, the image signal to noise ratio as defined is of more importance than displayed target to background contrast.

For a given target, the SNR is determined by the detector instantaneous field of view, the detector integration time, the detector noise, spatial noise due to nonuniformities in the responsivity of the elements of the array and photon noise. For systems using autonomous processors to detect and track targets the SNR is the most important measure of the system's capability to perform detection and tracking since it will define the threshold setting which must be used for feature extraction.

The target to background contrast is obtained by considering a uniform background of amplitude c extending from $-\infty$ to $+\infty$ with a target of amplitude b extending from -a to +b. The target produces a positive contrast on the focal plane. The differential target to background signal is calculated by integrating the background flux over the active area of the detector and then integrating the blurred differential target to background signal over the active area of the detector. The formalism adopted here uses a detector instantaneous field of view (IFOV) which is defined by the detector pitch; ie. the IFOV subtended by the total detector site, and a fill factor to correct for the partial occupation of the detector site by the active area of the detector.

The differential target to background photon flux can also be calculated as the differential flux collected for an extended target reduced by the scaling factor which corrects for the effects of optical blurring. The flux distribution on the focal plane for the target and background together is

$$\sqrt{\frac{\alpha}{\pi}}.\left(\int_{-\infty}^{-a} c.\exp(-\alpha(x-\tau)^2).d\tau + \int_{-a}^{a} b.\exp(-\alpha(x-\tau)^2).d\tau + \int_{a}^{\infty} c.\exp(-\alpha(x-\tau)^2).d\tau\right)$$

which can be reduced to

$$\sqrt{\frac{\alpha}{\pi}}.\left(\int_{-\infty}^{-\infty} c.\exp(-\alpha(x-\tau)^2).d\tau + \int_{-a}^{a} (b-c).\exp(-\alpha(x-\tau)^2).d\tau\right)$$

and the scaling factor which corrects for the effects of optical blurring is only applied to the second integral in the expression.

For systems utilising staring focal plane detector arrays (FPDAs), the nonuniformity of the responsivity of the elements of the array creates 'fixed pattern' noise which reduces the target to background signal to noise ratio. The amplitude of the fixed pattern noise is dependent on the correction algorithm which is used to compensate for the nonuniformity[4]. The fixed pattern noise is not static for detector arrays such as the array used in the experiments conducted and the time evolution of the fixed pattern noise is dependent on the $^1/_f$ noise of the detector elements. With time, $^1/_f$ noise processes evolve and the apparent responsivities of the detectors in the array change. The effect of this evolution on the performance of an imaging system is a time dependent degradation of target to background contrast. Therefore, $^1/_f$ noise may have a significant effect on the apparent nonuniformity of the responsivity of the elements of the array and thus on the probability of the detection of features within an image. In the analysis presented here, however, the temporal evolution of $^1/_f$ noise will be ignored.

With this simplification, the major noise sources are photon noise and system noise contributed to by the detector noise, noise from the readout and conditioning circuits which process the detector output and (with the stated approximation) fixed spatial noise. The measurement of detector and readout circuit noise for staring focal plane detector arrays is difficult. It is not normally possible to measure the detector noise power spectral density and thus a noise analysis based on the use of noise power spectral density is often not practically realisable. Manufacturers often specify the number of noise carriers per pixel for a given stare time and this is a relatively straight forward measurement to make practically.

For systems using staring arrays which integrate the carriers generated in each detector, it is convenient to model the total system noise as an equivalent noise generator in the detector which produces a given number of noise carriers per unit time. The pixel noise can be conveniently modelled with this equivalent detector noise current which is integrated for the stare time.

If the stare time is t_s, then the total number of carriers generated by the incident photon flux and collected at a detector site when the target is imaged is

$$N_t = t_s.(n_t + n_a) \tag{20}$$

and the total number of carriers collected at a detector site when the background is imaged is

$$N_b = t_s.n_b \tag{21}$$

The contribution to temporal noise from the incident photon flux from the background, expressed as the rms number of carriers generated due to fluctuations in the photon flux, the average pixel photon noise when imaging the scene background, is

$$N_e = \sqrt{t_s.n_b} \tag{22}$$

If the detector equivalent noise current accumulated in the integrating capacitor is i_n, the total number of noise electrons per pixel for a stare time (integration time) of t_s is

$$N_e = \sqrt{t_s.n_b + (\frac{t_s.i_n}{e})^2} \tag{23}$$

where e is the electronic charge. The target to background SNR is then obtained as

$$SNR_t = \frac{N_t - N_b}{N_e} \tag{24}$$

As would be expected, SNR_t decreases with increasing range since ϕ_t approaches zero as atmospheric transmission decreases with range and ϕ_a approaches ϕ_b with increasing range.

7 SPATIAL NOISE

In the model described here, the effect of spatial noise in the image due to non-uniformities in the detector responsivities is accounted for by calculating an equivalent noise signal. The temporal variation of the spatial noise due to detector responsivity non-uniformities is ignored and the spatial noise is considered as a fixed pattern noise. The target position and motion within the image are random and the treatment of spatial noise in this manner will produce an acceptable prediction for the probability of track formation for a target in an image.

The FPDA sensor system includes a real time processor which performs correction for detector responsivity non-uniformity. The algorithms used are a two point correction algorithm or a non-linear three point correction algorithm[4] which provides a lower residual non-uniformity of responsivity. The residual non-uniformity is expressed in terms of a root mean square (rms) variation of the apparent temperature observed when imaging a uniform extended source. In the model described, this rms variation is expressed as an equivalent rms flux variation, and thus a rms variation in the number of carriers generated, which can then be directly added (in quadrature) to the photon noise and the system noise. The equivalent mean square variation in carriers due to spatial noise when imaging a uniform extended source is

$$n^2_{fpn} = (\frac{A_d.\pi}{4.F^2})^2 \frac{\sum_{all\_pixels} (\int_{\lambda_0}^{\lambda_\infty} \eta(\lambda).(L_{q,\lambda}(\lambda, T_{pixel}) - L_q(\lambda, T_{average})).\tau_O(\lambda)d\lambda)^2}{no\_pixels}.[sec^{-2}] \tag{25}$$

where T_{pixel} is the apparent temperature producing the observed pixel output, $T_{average}$ is the image average temperature and no_pixels is the number of pixels in the image, in this case the number of detectors in the array. Using $T_{average}+\delta T$ instead of T_{pixel} allows calculation of n_{fpn} from a knowledge of the residual detector responsivity nonuniformity when this is expressed as a rms image temperature variation. The number of noise electrons per pixel is then given by

$$N_e = \sqrt{t_s . n_b + n_{fpn}^2 + (\frac{t_s . i_n}{e})^2} \tag{26}$$

where t_s is the pixel integration time. For the detector array used, a detector responsivity nonuniformity producing a rms image temperature variation of 0.1 K is equivalent to a rms photocarrier variation of $1.8*10^8$ carriers/s. This approach provides a convenient method of including the spatial noise generated by residual nonuniformities in the responsivity of the detectors in the array after compensation has been applied for such nonuniformities in the overall noise.

8 OPERATION OF THE MODEL

In the model described, the rate of generation of carriers due to emission from the atmosphere along the line of sight in the absence of a target is first calculated using data obtained from LOWTRAN. This calculation is performed using the detector and optical system spectral response characteristics, the detector instantaneous field of view, detector fill factor (0.511 for the detector array used) and optical systems parameters such as the collecting aperture area. The integration time or stare time then determines the number of carriers accumulated per detector as the background signal. An additional component of photocarrier generation due to stray flux, obtained by measurement, is used to account for internal flux. The number of carriers generated per pixel per frame due to the background is, from before,

$$N_b = \frac{A_d . v . t_s . \pi}{4 . F^2} \int_{\lambda_0}^{\lambda_\infty} \eta(\lambda) . \varepsilon_b(\lambda) . \tau_O(\lambda) d\lambda \tag{27}$$

where υ is the detector fill factor. For the detector array and optical system used this is typically of the order of 10^7 electrons. The variance of the rate of generation of carriers is then calculated. This includes the contributions of photon noise, system generated temporal noise and spatial noise.

The rate of generation of carriers due to emission from the atmosphere along the line of sight between the sensor and the target in the presence of a target is calculated similarly.

The spectral rate of emission of photons from the target is then calculated and modified by the spectral transmission of the atmosphere and the system optics and by the detector spectral response. For this calculation, the pixel IFOV and detector fill factor are used and the result of the calculation of the number of carriers generated by the target is then added to the rate of accumulation of carriers due to emission from the atmosphere along the line of sight. For a given background radiance, the rate of accumulation of carriers due to emission from the target and intervening atmosphere determines the differential target to background signal. The calculation of the excess rate of accumulation of carriers when a target is present over the background rate alone is then modified by the correction factor for target size calculated for the known target size and range. The number of carriers generated per pixel per frame due to the target is

$$N_t = \kappa . \frac{A_d . v . t_s . \pi}{4 . F^2} \int_{\lambda_0}^{\lambda_\infty} \eta(\lambda) . (L_{q,\lambda}(\lambda, T) . \tau_A(\lambda) + \varepsilon_a(\lambda)) . \tau_O(\lambda) . d\lambda \tag{28}$$

where κ is the correction factor which accounts for the effect of the apparent size of the target[5]. The correction factor is used to estimate the range dependent apparent change in radiance for the target which results from the change in apparent size of the target with range. κ also accounts for the effect of blurring caused by the system optics and is given by

$$\kappa = \frac{1}{2\pi A_d} \int \int_{\sqrt{2\alpha}(x-\frac{0.5}{\beta})}^{\sqrt{2\alpha}(x+\frac{0.5}{\beta})} \exp(-\frac{\tau^2}{2}) d\tau . \int_{\sqrt{2\alpha}(y-\frac{0.5}{\beta})}^{\sqrt{2\alpha}(y+\frac{0.5}{\beta})} \exp(-\frac{\sigma^2}{2}) d\sigma . dA \qquad (29)$$

where the outer integral is taken over the area of the detector. This expression for κ is readily derived from equation 6 and is normalised to the detector active area. Using these expressions, the signal to noise ratio, the ratio of the differential target to background signal to the rms pixel noise, is then obtained.

The correction to account for the effect of optical blurring on the observed signatures of sources which have a spatial extent which is less than the detector IFOV is more significant than the correction which results from scaling the output by the ratio of the source image and the detector IFOV which is sometimes used to account for sub-pixel targets. The requirement to correct for optical blurring is demonstrated by the fact that, if blurring is ignored, the calculated detector signal for the detector array used will be 18 per cent greater than the observed signal for a square source and 35 per cent greater than the observed signal for a circular source when the source images have an extent on the focal plane of 20 μm.

In operation, the model may be used to calculate the voltage which will be observed at the output of the detector array when the system is imaging a specified source. The calculation is straightforward and relies on a knowledge of the integration capacitance on the focal plane and the charge transfer efficiency of the multiplexing and readout electronics. The charge transfer efficiency specifies the efficiency with which carriers are transferred from the photodiodes to the integrating capacitors and from there to the output terminal of the detector array.

The storage capacitance on the focal plane is specified by the manufacturer of the detector array. The charge transfer efficiency and the detector peak spectral quantum efficiency are not specified by the manufacturer and must be determined by measuring the output voltage observed for known source temperatures. Such measurements effectively provide estimates of the product of these terms. The validity of the model is not reduced by the lack of this data since these parameters are scaling factors only and do not affect the estimation of system signal to noise ratios or image contrasts.

9 SYSTEM SIMULATION

To illustrate the use of the model and the effect of target size and range on target detection probability a simulation has been run using the model with a FPDA which is sensitive to infrared radiation in the 8 μm to 12 μm spectral region with detector parameters reflecting those of detectors currently available. The detector is assumed to 'stare' at the target, no scanning effects are considered.

The simulation has been run using atmospheric data for a representative altitude with appropriate environmental parameters. Figures 4, 5 and 6 display the atmospheric transmission and emission data for the simulation. Figure 4 shows the variation with wavelength of the atmospheric transmission between the sensor and the source. Figure 5 shows the variation with wavelength of the emission in the direction of the sensor which arises from the atmosphere between the sensor and the source. This emission is not the total background emission since it arises only from the atmosphere between the sensor and the source and includes no contribution from the atmosphere beyond the source.

The 'background emission' is the total atmospheric emission in the direction of the sensor which arises from the atmosphere along the line of sight in the absence of the source. Figure 6 shows the variation with

wavelength of the background emission and shows the increase in the observed background emission with increase in range to the target. This increase is due to the fact that, for constant target and sensor altitudes, as the range to the target increases the line of sight from the sensor to the target is depressed towards the surface of the earth and thus intersects more of the atmosphere. The background radiation collected by the sensor determines the target to background contrast since for constant target temperature and range, as the apparent background temperature increases the differential target to background signal decreases. The data shown were obtained using LOWTRAN and converted to photon units as described previously.

In undertaking the analysis of the performance of any sensor where the sensor to target distance is large, the geometry of the sensor line of sight relative to the earth must be accounted for. For constant sensor and target altitudes relative to the earths surface the line of sight passes closer to the earth's surface as the range from the target to the sensor increases and thus the apparent background temperature rises. Figure 5 shows the increase in observed emission with increase in range to the target from the atmosphere between the sensor and the target.

There are four significant mechanisms which act to reduce target detection probability with increasing range for constant target and sensor altitudes;

- the decrease in apparent target size (the angular subtense of the target),
- the increase in emission from the intervening atmosphere,
- the increased absorption of target emission, and
- the increase in background atmospheric emission due to a lower line of sight.

Figure 7 shows the decrease in the target to background image contrast with and without the attenuation due to the decrease in apparent size of the source with increasing range. The standard definition for contrast (the ratio of the difference between the target and background signals to the background signal) is used. The decrease in the target to background image contrast is due to the decrease in the difference between the target signal and the background signal with range due to atmospheric effects and the decrease in apparent size of the target with range. The attenuation of the target signal due to the reduction of apparent target size does not commence until the range increases to a distance for which the apparent size is reduced to a size of the order of the system PSF. For ranges greater than this the peak target signal decreases rapidly with increasing range.

Figure 8 illustrates the decrease in differential target to background signal to noise ratio as calculated using the estimates of pixel noise obtained with and without spatial noise. The data with spatial noise have been obtained for a residual detector responsivity nonuniformity equivalent to an apparent rms scene temperature variation of 0.1 K.

10 CONCLUSION

The sensor system model described here has been used for the analysis of the performance of a FPDA based imaging infrared sensor. The model has been developed using a photon formulation in preference to an energy formulation since this is consistent with the use to which the results of the model are to be put and with the analysis of operation of photon detectors more effectively than the energy formulation. The model provides estimates of the differential target to background signal to noise ratio which accommodate the effects of apparent target size and spatial noise arising from detector responsivity nonuniformities. The model is suited to the prediction of the performance of staring IRFPDA based imaging sensors and the predicted differential target to background signal to noise ratio can be used to estimate the target detection probability for automated processors.

11 REFERENCES

1 W.L. Wolfe, G.J. Zissis (editors), '*The Infrared Handbook*', Office of Naval Research, Washington DC, 1985

2 G.A. Findlay, D.R. Cutten, 'Comparison of performance of 3-5 and 8-12μm infrared systems' *Optical Engineering*, December 1989, Vol 28 No 23 p5029-5037

3 A.M. Papoulis, '*Systems and transform with applications in optics*', McGraw Hill, New York 1968

4 G.V. Poropat, 'Nonlinear compensation for responsivity nonuniformities in cadmium mercury telluride focal plane detector arrays for use in the 8μm to 12μm spectral region', *Optical Engineering*, August 1989, Vol 28 No 8 p887-896

5 G.V. Poropat, 'The effect of system point spread function, apparent size and detector instantaneous field of view on the infrared image contrast of small objects', *Optical Engineering*, (accepted for publication) 1993.

This is a blank page

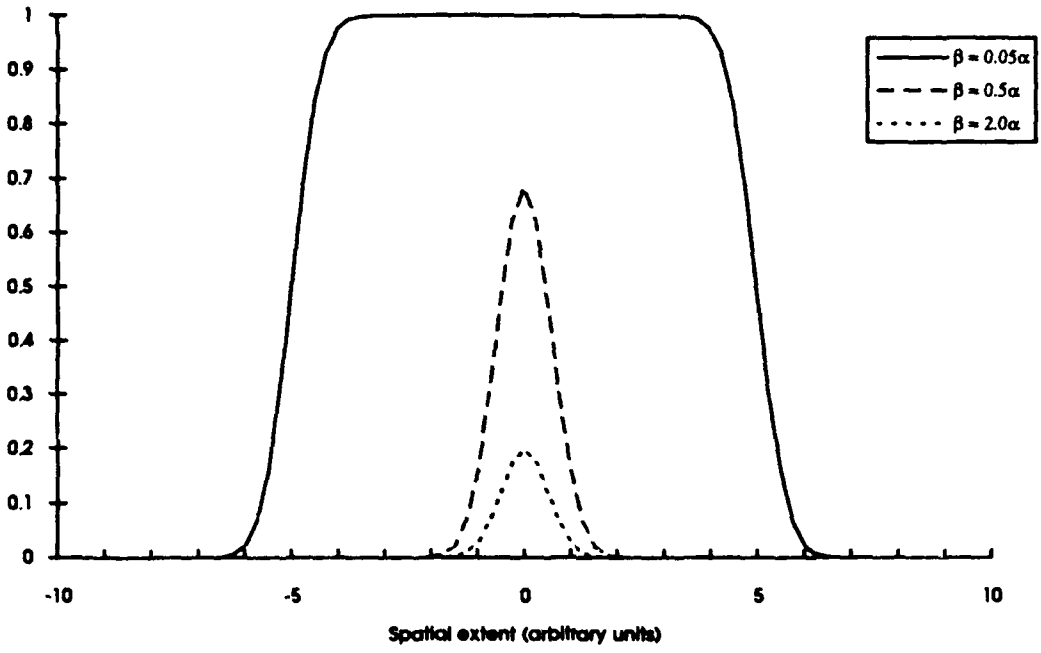

Figure 1: Variation of image amplitude with the apparent size of a line source

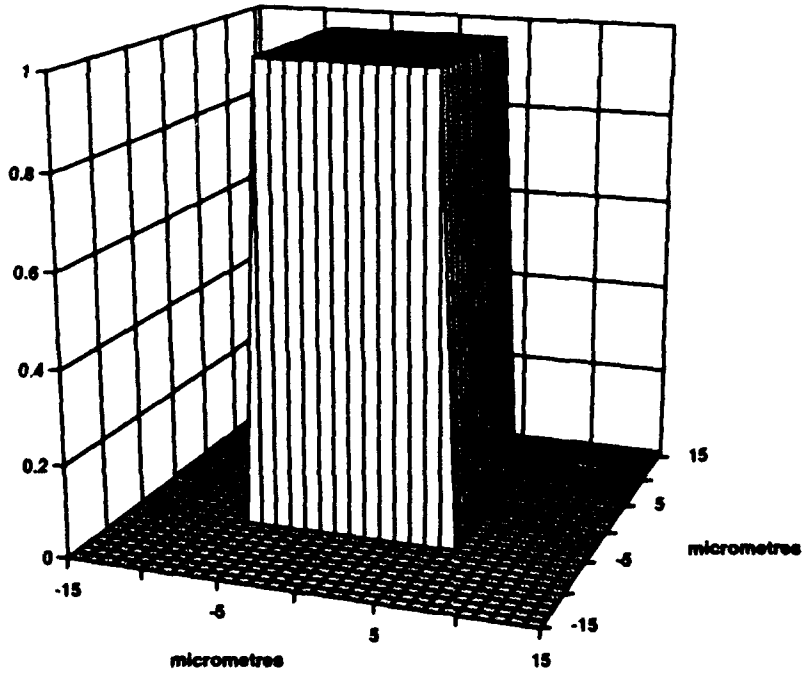

Figure 2: Unblurred square target image on the focal plane

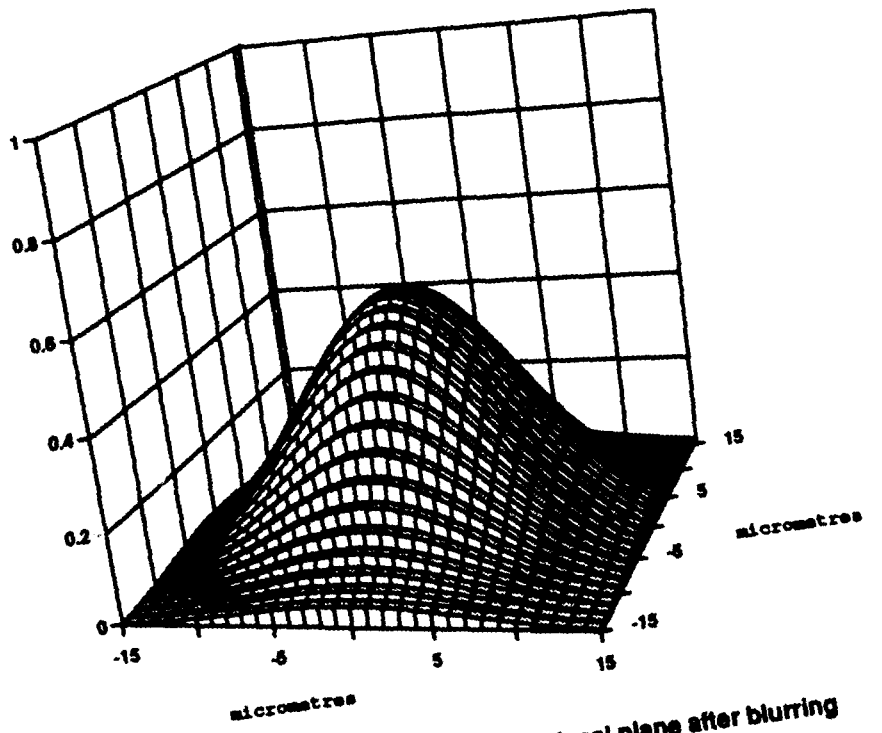

Figure 3: Square target image on the focal plane after blurring

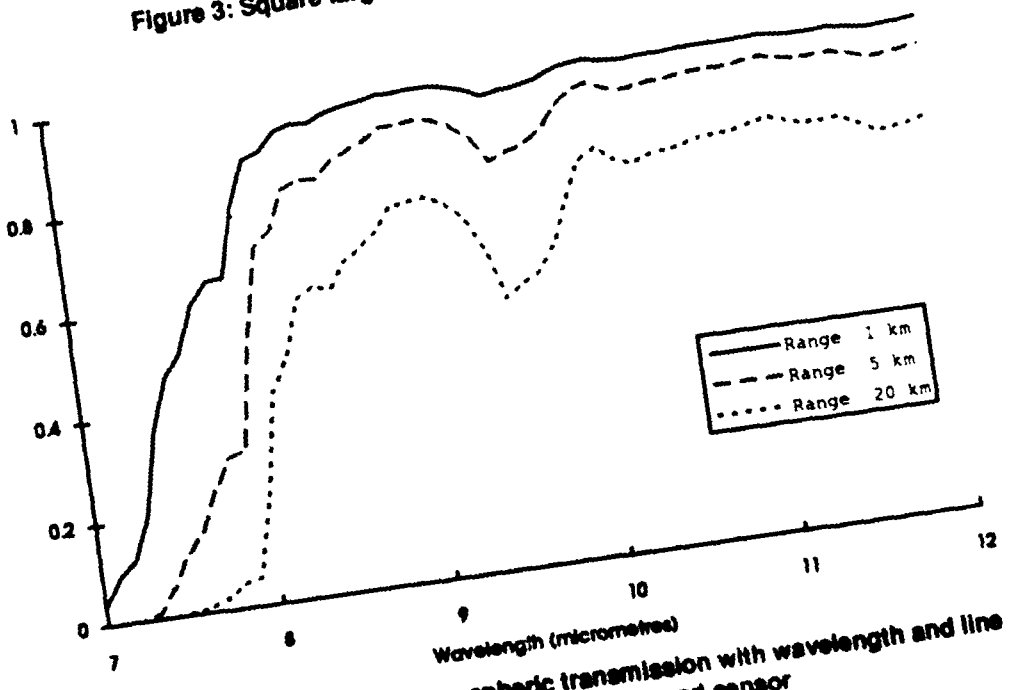

Figure 4: Variation of atmospheric transmission with wavelength and line of sight between source and sensor

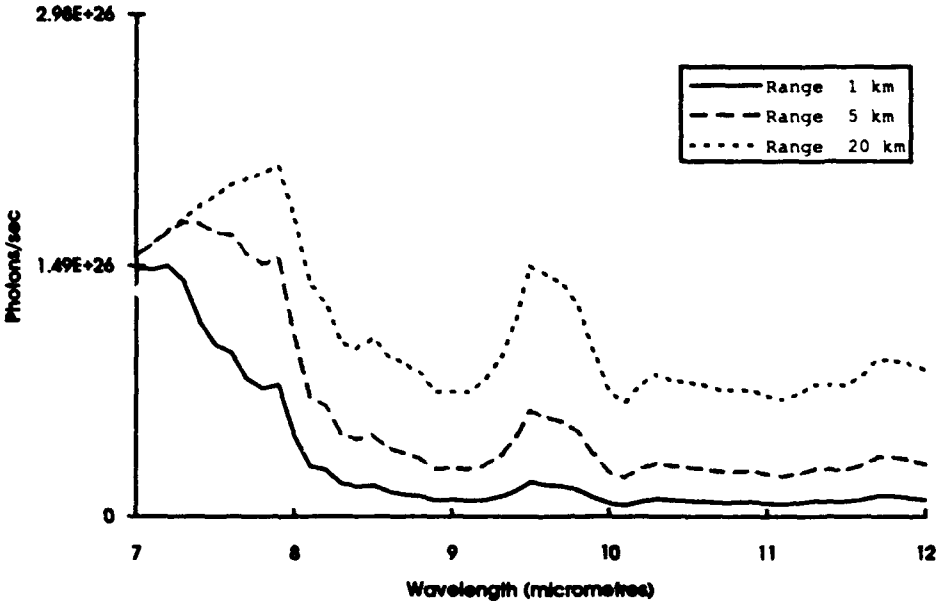

Figure 5: Variation of atmospheric emission between target and source along line of sight from sensor to target with wavelength and distance to source

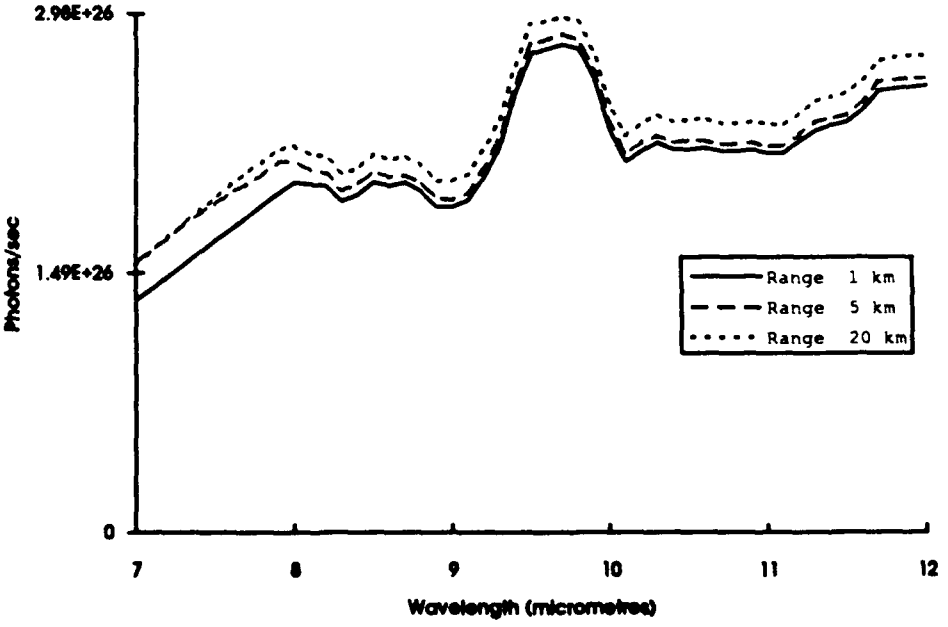

Figure 6: Variation of background atmospheric emission with wavelength and line of sight as determined by range to the target

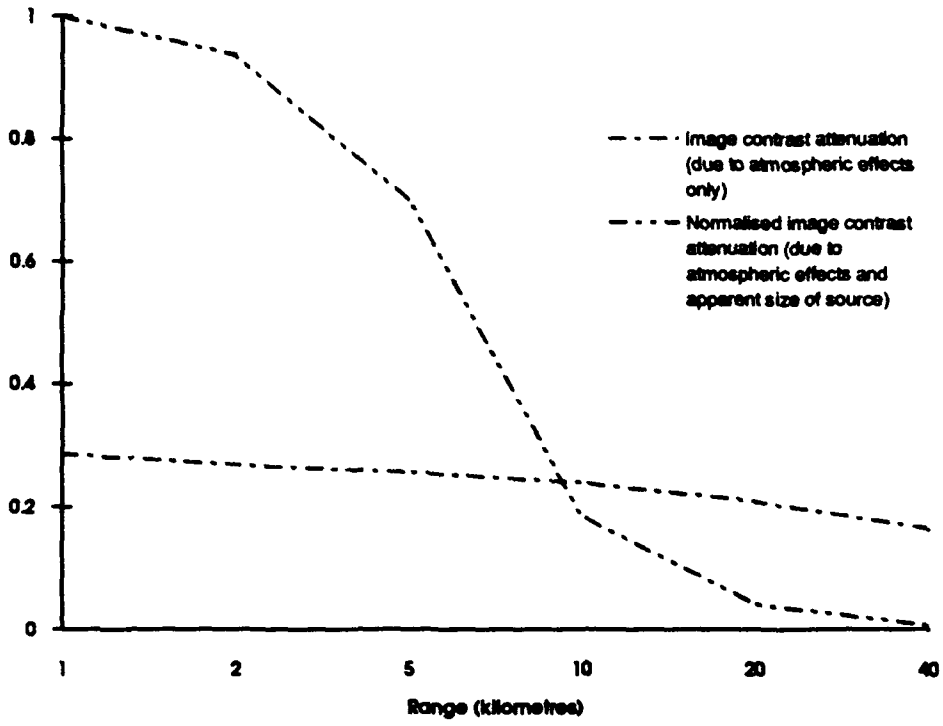

Figure 7: Image contrast attenuation due to the increase in atmospheric attenuation and the decrease in apparent size of source with increasing range to source

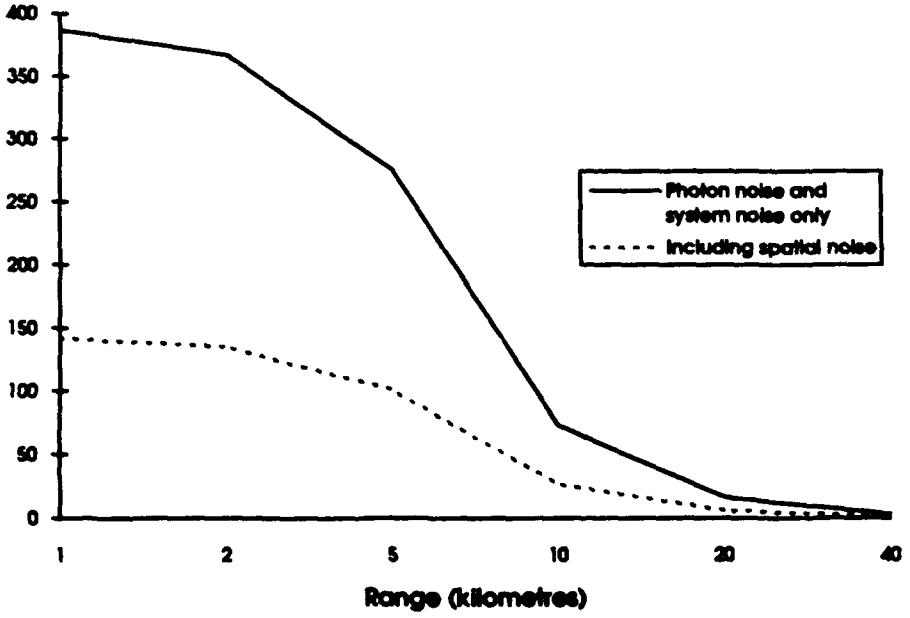

Figure 8: Variation of target to background differential signal to noise ratio with range to source

DISTRIBUTION

	Copy No.
Defence Science and Technology Organisation	
Chief Defence Scientist)	
Central Office Executive)	1
Counsellor, Defence Science, London	Cont Sht
Counsellor, Defence Science, Washington	Cont Sht
Scientific Adviser, Defence Central	1
Navy Scientific Adviser	1
Air Force Scientific Adviser	1
Scientific Adviser, Army	1
HQADF	
Director, Research Requirements Airforce	1
DDEW (Electronic Warfare)	1
Surveillance Research Laboratory	
Director	1
Chief, Optoelectronics Division	1
Research Leader, Optoelectronics Systems	1
Head, Systems Analysis	1
Head, Image Processing	1
Optoelectronics Division HQ	2
G.V. Poropat (Author)	2
Electronics Research Laboratory	
Head, Optoelectronic Warfare	1
Aeronautical Research Laboratory	
Dr O.M. Williams	1
Libraries and Information Services	
Australian Government Publishing Service	1
Defence Central Library, Technical Reports Centre	1
Manager, Document Exchange Centre, (for retention)	1
National Technical Information Service, United States	2
Defence Research Information Centre, United Kingdom	2
Director Scientific Information Services, Canada	1
Ministry of Defence, New Zealand	1
National Library of Australia	1
Defence Science and Technology Organisation Salisbury, Research Library	2
Library Defence Signals Directorate, Melbourne	1
British Library Document Supply Centre	1
Defence Intelligence Organisation Research Service	1
Spares	
Defence Science and Technology Organisation Salisbury, Research Library	6
	Total 39

Department of Defence

DOCUMENT CONTROL DATA SHEET

Page Classification	
UNCLASSIFIED	
Privacy Marking/Caveat (of Document)	
N/A	

1a. AR Number	1b. Establishment Number	2. Document Date	3. Task Number
AR-008-151	SRL-0112-RN	December 92	ADA 87/026

4. Title

SENSOR MODELLING FOR THE 'CYCLOPS' FOCAL PLANE DETECTOR ARRAY BASED TECHNOLOGY DEMONSTRATOR

5. Security Classification

Document	Title	Abstract
U	U	U

S (Secret) C (Confi) R (Rest) U (Unclass)

* For UNCLASSIFIED docs with a secondary distribution LIMITATION, use (L) in document box.

6. No. of Pages	30
7. No. of Refs.	5

8. Author(s)

G.V. Poropat

9. Downgrading/Delimiting Instructions

N/A

10a. Corporate Author and Address

Surveillance Research Laboratory
PO Box 1500
SALISBURY SA 5108

10b. Task Sponsor

DGFD(Air)

11. Officer/Position responsible for

Security.....

Downgrading.....

Approval for Release.....DSRL.....

12. Secondary Distribution of this Document

APPROVED FOR PUBLIC RELEASE

Any enquiries outside stated limitations should be referred through DSTIC, Defence Information Services, Department of Defence, Anzac Park West, Canberra, ACT 2600.

13a. Deliberate Announcement

No limitation

13b. Casual Announcement (for citation in other documents)

[ ] No Limitation

[√] Ref. by Author , Doc No. and date only.

14. DEFTEST Descriptors

Infrared detectors, Focal plane arrays, Performance evaluation, Mathematical models

15. DISCAT Subject Codes

170501

16. Abstract

The Surveillance Research Laboratory of the DSTO has developed a technology demonstrator utilising an infrared focal plane detector array to assess the feasibility of using large scale infrared detector arrays for ADF applications. The imaging sensor which has been developed requires no scanning mechanism and uses an array of mercury cadmium telluride detectors sensitive to radiation in the 8 μm to 12 μm spectral region to produce an image. The sensor was tested in a series of airborne trails and the results obtained from these trials will be used to evaluate the performance of focal plane detector array based systems. A mathematical model of the sensor has been used to evaluate the performance of the sensor. The mathematical model has been developed to meet the requirements imposed by analysis of the performance of this sensor. The model is based on the description of the operation of the elements of the detector array as photon counters. A description of the model used for the analysis of the data obtained using the sensor is presented here.

Page Classification
UNCLASSIFIED

16. Abstract (CONT.)

17. Imprint

Surveillance Research Laboratory
PO Box 1500
SALISBURY SA 5108

18. Document Series and Number	19. Cost Code	20. Type of Report and Period Covered
SRL-0112-RN	807319	RESEARCH NOTE

21. Computer Programs Used

N/A

22. Establishment File Reference(s)

N/A

23. Additional information (if required)